Journal of Electronic Materials, Vol. 13, No. 1, 1984

CHARACTERIZATION OF TERNARY Cu-Sn-Au BULK ALLOYS AND THIN FILMS

J. Kim

IBM, Thomas J. Watson Research Center
Yorktown Heights, New York 10598

(Received March 24, 1983; revised October 3, 1983)

The variation of the microstructure and corresponding properties of several Cu-based Au alloys with differing Sn contents was investigated. Both bulk alloys and thin films of the same composition were studied to determine whether characterization of the bulk alloys could be used to predict the optimal thin film composition. For bulk alloys with less than 10% Sn content, the electrical resistivity and hardness were found to be only slightly increased over those of a Cu-Au alloy with no added Sn ; however they increase rapidly with further increases in Sn content. A microstructural study indicated that these changes in properties are primarily attributable to the formation of a hard ε-Cu_3Sn phase. The characteristic needle shape of these preciptated particles, as well as their volume fraction, seems to contribute to the embrittlement of the alloy. The orientation relationship between α-Cu and the ε-Cu_3Sn precipitate was found to be $[1\bar{1}0]_\alpha // [0001]_\varepsilon$, $\{111\}_\alpha // (10\bar{1}0)_\varepsilon$, and $(\bar{1}\bar{1}3)_\alpha // (1\bar{2}10)_\varepsilon$. The relative variation in resistivity as a function of Sn concentra-

0361-5235/84/1301-0191$3.00

tion was the same for the thin film and the bulk alloy, although their absolute values were different because of surface oxidation and small grain size in thin films. Given the observed microstructural similarity, the similar composition dependence leads to the conclusion that the properties of bulk alloys may be used to make reasonable predictions about the behavior of thin films in systems in which the thin film phase composition is the equilibrium one by heat treatment.

Key words: Cu-Sn-Au alloy, ε-Cu_3Sn phase, orientation relationship, electrical resistivity.

Introduction

As thin film technology has become more important to the packaging of microdevices, soldering materials for thin film interconnection junctions have become critically important to the electronic industry (1,2). The design of these junctions requires a knowledge of the correlation between the composition of the thin film and its properties. However, in thin films this relationship is often obscured by thickness effects and other variables (3,4). Analysis is also complicated by the variety of nonequilibrium structures which may appear with slight variations in processing. Since it is easier to study isolated parameters in bulk materials, design of interconnection junctions is greatly facilitated if the structure and property of the thin film could be correlated with those of bulk alloy.

This work was conducted to investigate the similarity of a thin film junction structure and its properties to those of bulk alloys of the same composition. An entire system must be studied since it is the intermetallic compound formed by the reaction of the soldering material with the basic

conducting line, not the soldering material itself, which determine the structural soundness of the junction (5-7). The Cu-Sn-Au ternary alloy system was selected for this study because it is the simplest practical system for junction structure, namely, Cu for conducting line, Sn for soldering material, and Au to prevent oxidation. All of the experimental variables in this experiment, such as film thickness and heat treatment, were chosen to be as close as possible to those currently applied for microdevice interconnection.

The physical and mechanical properties of Cu based Sn alloys have been well established elsewhere (8). However, those of the ternary alloy with substitutional Au have not. Accordingly, structural studies of the alloys were carried out using transmission electron microscope and x-ray diffractometer. The hardness, soldering strength, and electrical resistivity were measured for the bulk alloys. Resistivity was chosen for comparison between thin film and bulk alloy because it is the only one of these properties for which testing technique may be eliminated as a variable between both types of specimens. Finally, the measured properties were correlated with the observed microstructures.

Experimental Procedure

The Cu-Sn-Au bulk alloys were prepared in an arc-melting furnace and then homogenized under vacuum at 700 C^0 for 28 hours. The final chemical compositions of the alloys were Cu + 1.0%Sn + 0.8% Au, Cu + 4.3%Sn + 1.2%Au, Cu + 9.7%Sn + 0.9%Au, and Cu + 24.6%Sn + 1.2%Au in weight percent. The ingots were forged and then annealed at 700 C^0 for 2 hours under vacuum. Finally the annealed alloys were cut to the testing size and further annealed at 250 C^0 for 30 minutes.

The thin film specimens, 5 μm trilayer of Cu, Sn, and Au, were made by e-beam evaporation through a molybdenum mask onto aluminum oxide substrates. These depositions were made at 220 C^0, 25 C^0, and -110 C^0, respectively. The Sn and Au were deposited at low temperature to prevent possible interdiffusion or diffusion into Cu. All the samples had a layer of Sn between Cu and Au layer. The thickness of each layer was carefully controlled so that the final film compositions were basically same as those of the bulk alloys, i.e., 1%Sn, 4%Sn, 10%Sn, and 25%Sn Cu+1%Au alloys. Two identical thin film structures were sandwiched and then annealed at 250 C for 30 min. at a pressure of 100 psi to make a junction structure. For transmission electron microscopic study, 1800 A thick trilayers of Cu-Sn-Au of the same compositions as those on ceramic substrates were evaporated on Si_3N_4 windows and annealed at 250 C for 1, 10, and 30 min.

Electrical resistivity measurements of both the bulk alloys and the thin films were conducted using 4-probe technique at a constant current of 100 mA. To check the distribution of resistance, for the 10 μm junction, all of the 36 pads made in a single deposition through Mo mask were tested. It was not possible, however, to determine the resistivity of the junctions because the thickness and the exact contact area of the junction were not measurable. Hardnesses of the bulk alloys were measured on a Brinnel Hardness scale. Samples for the soldering contact strength test of the bulk alloys were made by joining two sections with a cross-section of 1 cm x 0.25 cm with 40-60 Sn-Pb solder at 250 C. The soldered pieces were then pulled in an Instron Tensile testing machine. All microstructural analysis including phase analysis was done using an x-ray diffractometer and a JEOL 200B transmission electron microscope with a 200 KV accelerating voltage.

Result and Discussion

Microstructure and property of bulk alloy.

The microstructure of the 1%Sn alloy is shown in Figure 1. Its structure is clean and dislocation free. As is typical for a face centered cubic structure, many fine annealing twins with [111] twinning axis were present in the grains. In agreement with the Cu-Sn phase diagram, no precipitates were found in this alloy by either TEM study or

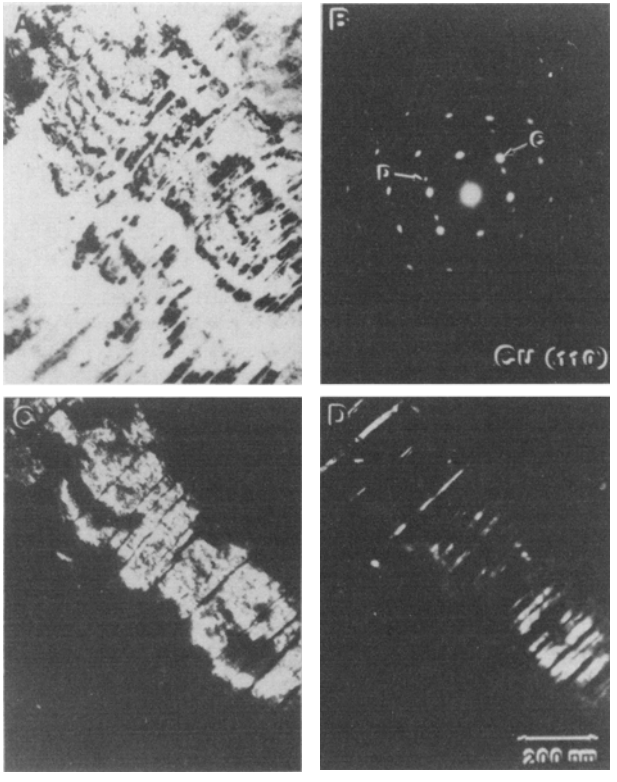

Fig. 1. Transmission electron microstructure of the 1%Sn alloy; (A) Bright Field, (B) Diffraction pattern, (C),(D) D.F. from spot c, d, in (B).

optical study. The grain size was about 150 μm for all the bulk alloys.

As illustrated in Figure 2, when the Sn content of the alloy was increased to 4.3%, precipitation of the long-range ordered ε-Cu_3Sn phase was observed. The volume fraction of the ε-phase was found to be less than 1% by optical microscopy. In the 10%Sn alloy, this volume fraction increased to around 9%. As shown in Fig. 3, the precipitate was always plate-shape and the orientation relationship between the α-Cu matrix and the ε-Cu_3Sn phase was found to be $[1\bar{1}0]_\alpha // [0001]_\varepsilon$, $(\bar{1}\bar{1}1)_\alpha // (10\bar{1}0)_\varepsilon$, $(\bar{1}\bar{1}3)_\alpha // (1\bar{2}10)_\varepsilon$, where ε-$Cu_3Sn$ phase was indexed as a pseudo-hexagonal close-packed system. It should be noted that although the close packed planes of the α and the ε phases are not parallel, the interplanary spacings are well matched by this orientation relationship. Although the formation of Au-Sn intermetallic compounds is known to be energitically more favorable than the formation of Cu-Sn intermetallics (9), ε-Cu_3Sn phase was the only precipitate detec-

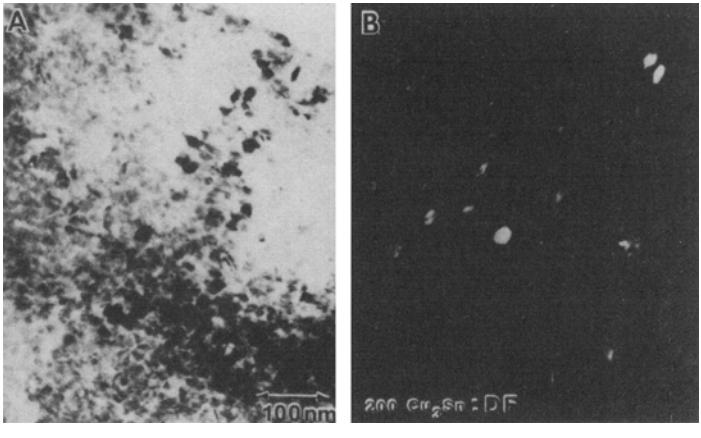

Fig. 2. TEM microstructure of the 4% Sn alloy, (A) Bright Field and (B) Dark Field of ε phase.

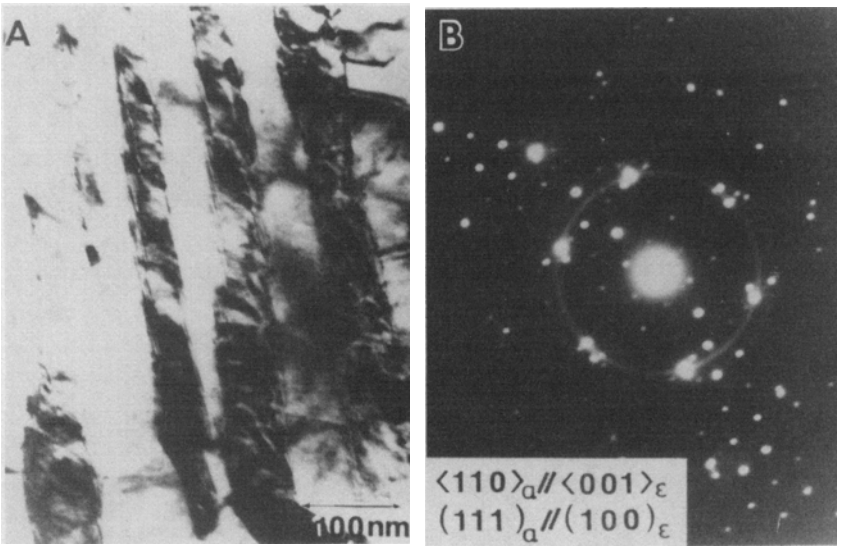

Fig. 3. TEM microstructure of the 10% Sn alloy. (A) B.F. and (B) corresponding diffraction pattern.

ted by both x-ray and electron diffraction studies. A possible explanation for this result is that Au-Sn compounds were in fact present, but in amounts too small to be detected by the analysis.

Figure 4 shows a typical microstructure and corresponding diffraction pattern of the 25%Sn alloy. Like the low Sn alloys, the 25%Sn alloy was composed exclusively of a α-Cu and ε-Cu_3Sn phases. However, in agreement with the binary phase diagram, ε-phase was the major phase and α-phase was minor. The alloy was estimated to be 60% ε-phase by optical microscopic study. Fine, sharp plates of ε-Cu_3Sn phase were visible within the islands of α-Cu phase indicating a continuous phase transformation to ε-Cu_3Sn during the annealling at 250 C. As shown in the figure, the orientation relationship between α-Cu phase and ε-Cu_3Sn phase was the same as for the low Sn alloy in which

α-Cu was the major component.

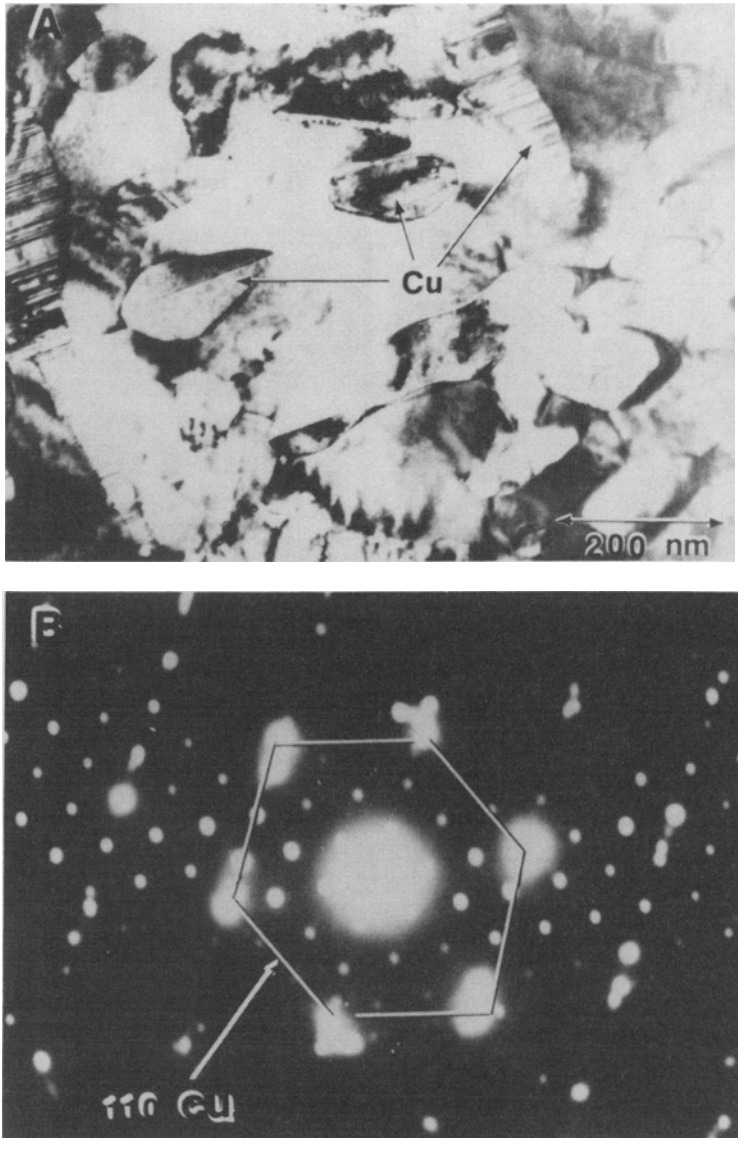

Fig. 4. TEM microstructure of the 25%Sn alloy, (A) B.F. and (B) corresponding diffraction.

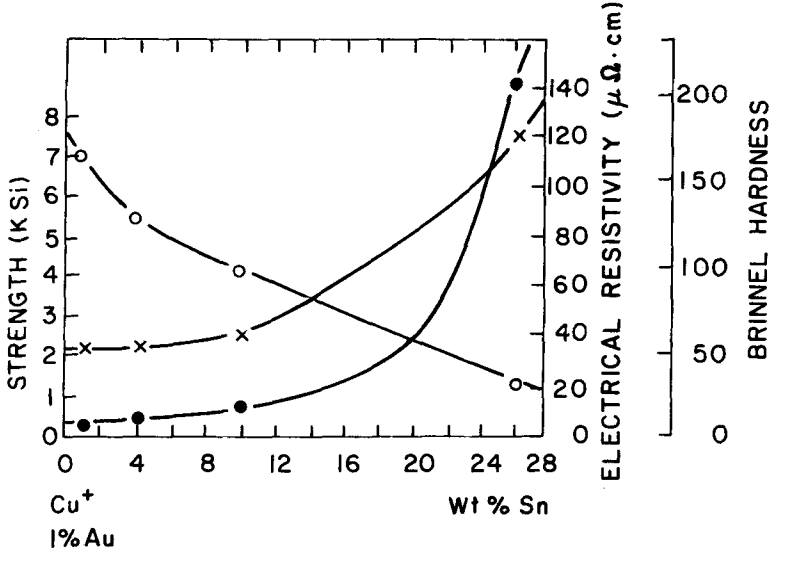

Fig. 5. Changes in properties of the alloys as a function of the Sn content. x shows hardness, dot represents electrical resistivity, and open circle shows soldering strength.

The changes in hardness, electrical resistivity, and soldering contact strength as a function of the Sn content of the bulk alloy are illustrated in Figure 5. Both the hardness and the electrical resistivity of the alloys increased with Sn content; however this increase was not proportional to the volume fraction of the ε-phase as might have been predicted. Instead, the values were only slightly higher for Sn contents under 10% and increased rapidly for further Sn additions. Thus, the hardness of the 10%Sn alloy was almost the same as that of the 1%Sn alloy, whereas the electrical resistivity of the 25%Sn alloy was approximately 20 times that of the 10%Sn alloy. The soldering contact strength of the alloys decreased, on the other hand, monotonically with Sn content.

The detailed experiments required to formulate the properties of the Cu-Sn-Au alloy system as a function of either the Sn content or the ε-Cu_3Sn volume fraction were not performed as part of this work since the primary objective was to compare the structure and properties of the bulk alloys and the thin films. The coherency of the second phase with respect to the matrix and their interspacing, size of the precipitate, and shape of the precipitate must be throughly investigated to reach a complete understanding of the effect of the ε-phase on the properties of the alloy, since all of these characteristics of the precipitate play a role in determining the final properties (10-12). It does seem clear, however, that volume fraction of the ε-Cu_3Sn phase is not the sole reason for the greater hardness of the high-Sn alloys. Since crack propagation is greatly facilitated along the boundary of a plate-shaped precipitate (12), the needle-shape of the precipitate of ε-Cu_3Sn is probably responsible for much of the embrittlement of the alloy and, therefore, for the rapid hardness increase with respect to the Sn concentration.

Microstructure and property of thin film.

Figure 6 shows the diffraction pattern of the thin film trilayer of Cu, Sn, and Au in an as-deposited condition and after 30 min. annealing at 250 C. The corresponding microstructural changes during the annealing process may be seen in Figure 7. In the as-deposited condition, the diffraction from each unreacted element is superimposed. During annealing some of the Sn melted, resulting in a fluxless soldering of the layers in the film. As shown in Figure 6, the main diffraction from the annealed film was from the newly formed ε-Cu_3Sn phase; however, a weak pattern from pure Cu is still apparent. The diffraction pattern from the annealed sample could be indexed to reveal weak diffractions from pure Au as well, since all the

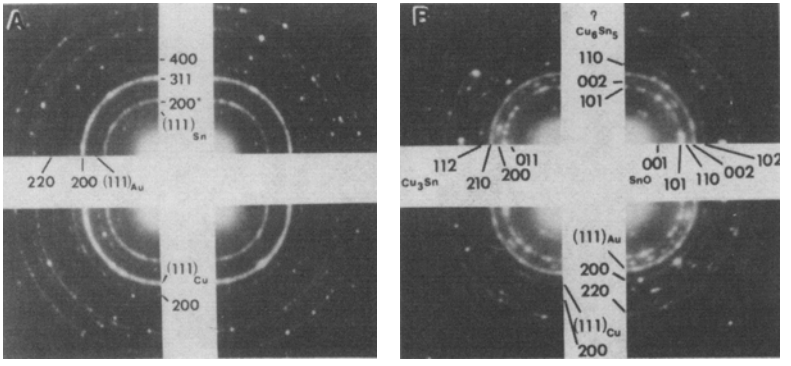

Fig. 6. Diffraction pattern of thin film before annealing (A) and after annealing (B).

primary diffractions of the pure Au would be very close to those from ε-Cu_3Sn phase and to those from SnO phase. However, it is highly unlikely that any pure Au would remain after annealing at 250 C. There is no diffraction evidence for the formation of Au-Sn intermetallic compounds, but since Au is more reactive with Sn than Cu (9), it it probably reacted completely with Sn. Due to the small initial concentration of Au, these phases might not be detectible by the electron diffraction even if they had formed.

The microstructure of the thin films was almost identical to that of the bulk alloy. The major diffrence between them was that the grain size of the thin film structure was about 0.2 μm, extremely small in comparison to the 150 μm grain size typical of the bulk alloys. The phase composition was the same in both structures except that in the thin films SnO was also present. As will be discussed later, the SnO phase seems to have an important role in determining the properties of the thin film. The presence of another Cu-Sn intermetallic compound, η-Cu_6Sn_5 phase, in the thin film structure is also possible, since the diffraction rings

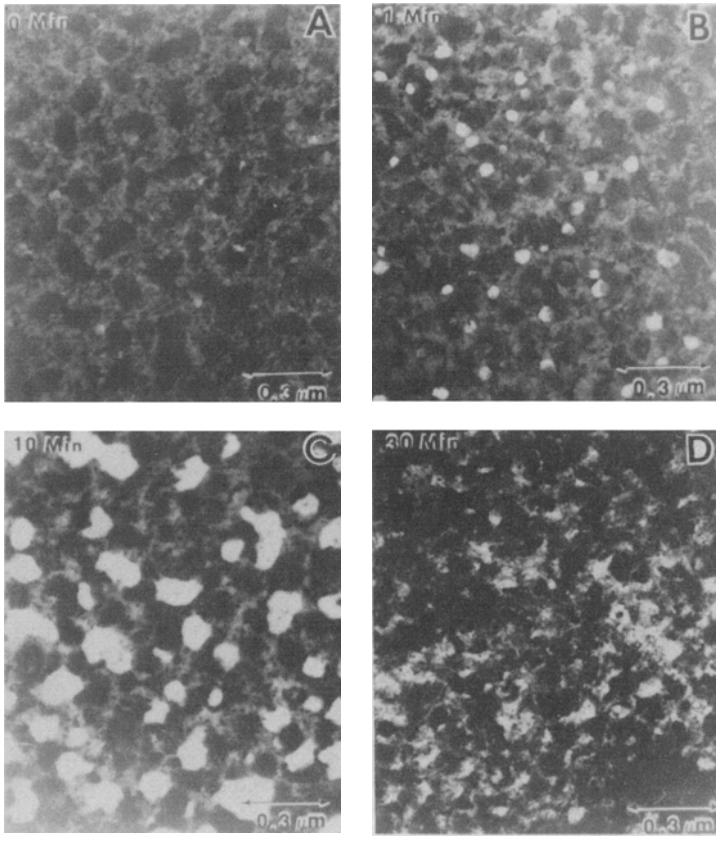

Fig. 7. TEM microstructure of the thin film, (A) as-deposited, (B) after 1 min. annealing, (C) after 10 min., and (D) after 30 min. annealing.

from the η-Cu_6Sn_5 phase would be superimposed on diffraction rings from the SnO phase. However, its presence is unlikely; it has been found previously (13) that annealing above 100 C does not favor a formation of the η-Cu_6Sn_5 phase.

Figure 8 is a cross-section of a thick film pad of Cu-Sn-Au trilayer on ceramic substrate which was annealed for 30 min. at 250 C. Also included are x-ray maps showing the distribution of

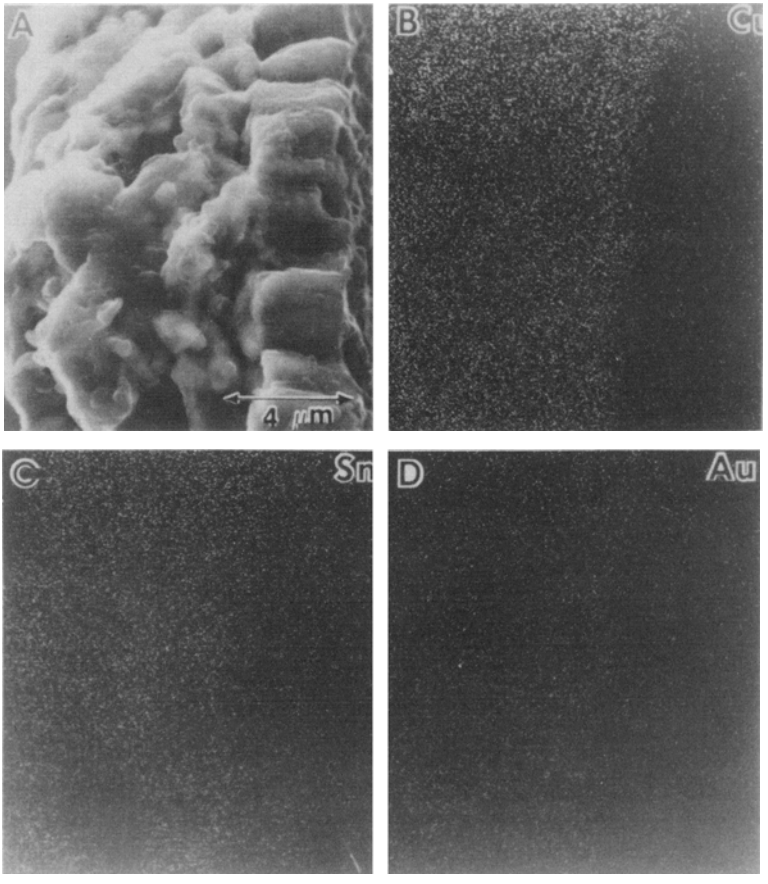

Fig. 8. SEM cross-sectional structure of the thick film junction pad (A) and (B),(C),(D) are x-ray maps of Cu, Sn, and Au, respectively.

each element. As indicated by the maps, all three elements were distributed uniformly through the 10 μm thickness. X-ray diffractometric analysis of the mixture showed that the structure was mainly ε-Cu_3Sn with a small amount of residual α-Cu phase interspersed. An attempt to cónfirm the presence of Au-Sn intermetallic compounds was not succesful for these samples either, again probably due to their very low concentration rather

than their complete absence. Unlike the thin film layers on Si_3N_4 windows, the thick film structure did not contain a detectable amount of SnO. This difference could be a result of changed experimental procedure; the thick film structure was annealed after the thin film pads were sandwiched together so that there was no free Sn surface. The absence of SnO means that except for its small grain size, which was the same as that of the thin film specimens, the thick film junction structure was identical to that of the bulk alloys.

The electrical resistivities of the thin films before and after annealing are shown in Table I. Also given is the distribution of resistances among the thick film junction pads. The unusually high resistances were found to correspond to samples in which the junction was poor and its cross-section small. In the as-deposited condition the electrical resistivities of the thin films were almost independent of Sn content. Cu, as the top layer on all the junction pads, was the actual contact for the four probes used for the resistivity measurement, so these values probably represent the resistivity of the pure Cu. Annealing at 250 C for 30 min. altered the resistivity of all the films. As

Table I. Electrical Properties of Thin Film Samples.

		1%Sn	4%Sn	10%Sn	25%Sn
As-deposited(1)		96	108	105	102
After anneal(1)		520	650	790	8700
Thick film junction (2)	(a)	#19	#18	#22	#0
	(b)	#13	#14	# 9	#12
	(c)	# 4	# 9	# 5	#15
	(d)	# 0	# 0	# 0	#9

(note) (1) resistivity (nano-ohm-m) of thin film.
(2) Number of pad of which resistance(milli-ohm) is (a)$\leq$1, (b)$\leq$5, (c)$\leq$10, and (d)$>$10.

As shown in the table, for Sn contents up to 10%, the resistivities were only slightly increased. However, the resistivity of the 25% Sn sample was a factor of 10 greater than that of the low Sn films. The absolute values of the resistivities of all the Sn films were about 10 times greater than those of the bulk alloys of the same composition; however, the relative resistivity values for the various Sn contents were comparable. As will be discussed later, the disagreement probably arises from the two major differences in the microstructures of the thin films from the bulk alloys, small grain size and the presence of SnO.

Comparison of thin films to the bulk alloys

After annealing at 250C, both the thin and thick film junction structures and the bulk alloys consist largely of α-Cu phase and ε-Cu3Sn phase. The only observed microstructural differences between them were the formation of SnO in the thin film structure and the very small grain size of the thin and thick film structures. The relatively large grains of the bulk alloys are obviously due to grain growth during the long initial annealing at 700C prior to the precipitation of the ε-Cu3Sn phase at 250C. The much smaller grain size of the thin films is only a result of the different heat treatment they received. The SnO oxide phase appears to be formed at or near the surface of both the bulk alloys and the thin films. However, since the surface to volume ratio is much smaller for the bulk alloy, the oxide layer could easily go undetected in the bulk alloy while being clearly observed in the thin film structure. Surface oxidation can be prevented; there is no evidence for the formation of SnO in the thick film junction, in which the Sn is not exposed. It may be concluded that both the small grain size and the Sn oxidation of the thin film structure are results of the experimental conditions, not the intrinsic properties of the films.

There is another mechanism which can cause the properties of thin films to differ from those of bulk alloys. It is well known that there is a critical film thickness below which the properties of a thin film are altered from those of a thick film or bulk alloy (14). The critical thickness depends on the property of interest, varying from 15nm for flow stress to 1000Å for electrical resistivity (15, 16). In this work, the electrical resistivity measurements were conducted on thin films 1800Å in thickness and 10μm thick films. The thicknesses of both types of films are significantly greater than the critical thickness for electrical resistivity reported by Mayer (15). The measurements in Table I can therefore be considered to be free of thickness effects.

As mentioned earlier, the major distinctions in the microstructures of the thin films from the corresponding bulk alloys are the presence of SnO and the much smaller grain size. Since the microstructures are basically identical in other respects and since the thickness effect may be neglected, the discrepancy between the absolute resistivity values must be due to one or both of these differences. Therefore, comparisons of the absolute values are meaningless, since these factors which cause them to disagree are controlled by the experimental conditions, not the intrinsic characteristics of the film. However, while it is not reasonable to compare the absolute values of the resistivities to those of the thin films, it is valid to compare their relative variations as a function of Sn concentration. If such a comparison is made it can be seen that the changes in resistivity are the same for the thin films, thick films and bulk alloys.

Summary

Two major conclusions about the Cu-Sn-Au ternary alloys system may be reached on the basis of this investigation.

From an alloy design perspective, low Sn alloys appear to have the best combination of properties. They are less resistant to electrical current, less brittle, and have better soldering characteristics than the high Sn alloy. These properties change drastically for the worse if the Sn content exceeds 10%. The increased hardness of the Cu alloy with the addition of Sn is attributed primarily to the formation of hard ε-Cu_3Sn precipitates and secondarily to the needle shape of the precipitate which facilitates crack propagation. The orientation relationship of the ε-Cu_3Sn phase with respect to the α-Cu is $\langle 110\rangle\alpha // \langle 0001\rangle\varepsilon$ (111) α//(10$\bar{1}$0) ε, and (113) α// (12$\bar{1}$0) ε.

The structure of the annealed thin film is quite similar to that of the bulk alloy. Consequently, the variation in resistivity as a function of Sn content is the same in thin films as in bulk alloys, although the absolute values differ as a result of the microstructural differences that do exist, the small grain size and SnO phase of the thin film. On this basis it may be concluded that other properties of the thin film could be predicted from the properties of the bulk alloy if allowance were made for the differences in microstructure. More generally, it may be concluded that in systems in which the thin film phase composition is the same as the equilibrium phase composition, the variation in thin film properties with various parameters may be extrapolated from the behavior of the bulk alloys.

Acknowledgement

The author is thankful to Drs. C. W. Ho and S. H. Wen for their support and discussion. He wishes to thank D. Yee, T. McCarthy, M. A. Tumolo and J. Glazer for technical assistance.

References

1. A. J. Blodgett, Jr., IEEE Trans. on Component, Hybrids, and Manufacturing Tech. 3, 634 (1980).

2. E. T. Lewis, IEEE Trans. on Component, Hybrids, and Manufacturing Tech. CHMT-2, 441 (1979).

3. D. S. Campbell, Mechanical Properties of Thin Films in Thin Film Technology, edited by L. I. Maissel and R. Glang, 1970, McGraw-Hill Co., Chap. 12.

4. L. I. Maissel, ibid, Chap. 13.

5. L. F. Miller, IBM J. Res. and Dev. 13, 239 (1969).

6. L. S. Goldman, R. J. Herdzik, N. G. Koopman, and V. C. Marcott, Proc. of the 27th Elect. Comp. Conf., Arlington, VA. May 16-18, 25 (1977).

7. R. T. Howard, IBM J. Res. and Dev. 26, 372 (1982).

8. Property and Selection: Nonferrous Alloys and Pure Metals, Metal Handbook, 9th ed. 2, ASM.

9. R. Holtgren, R. L. Orr, P. D. Anderson, and K. K. Kelly, "Selected Values of Thermodynamic Properties of Metals and Alloys", John Wiley & sons, Inc. N.Y. 1963.

10. A. R. Rosenfield and G. T. Hahn, Proc. of the Conf. on Physical Basis of Yield and Fracture, London, 47 (1966).

11. N. S. Stoloff, "Fracture", edited by H. Liebowitz, Vol. VI, Academic Press, N.Y., 22 (1969).

12. E. C. Bain and H. W. Paxton, "Alloying Elements in Steel" 2nd ed., ASM, Cleveland, 38 (1962).

13. K. N. Tu, Acta Met. 21, 347 (1973).

14. J. W. Menter and D. W. Pashley, Proc. of the Int. Conf. on Structure and Property of Thin Film, Bolton landing, N.Y., Sept. 9-11, 111 (1959).

15. H. Mayer, ibid, 225.